This is to certify that the

thesis entitled

Finite Element Method Applied to Deformation of
Metallic Glass Ribbon Reinforced Glass - Ceramic Matrix
Composite Material
presented by

John Dung Ninh

has been accepted towards fulfillment
of the requirements for

Master's _degree in Metallurgy

Major professor

Date 4/10/91

PLACE IN RETURN BOX to remove this checkout from your record.
TO AVOID FINES return on or before date due.

DATE DUE	DATE DUE	DATE DUE
_____	_____	_____
_____	_____	_____
_____	_____	_____
_____	_____	_____
_____	_____	_____
_____	_____	_____
_____	_____	_____

MSU Is An Affirmative Action/Equal Opportunity Institution

c:\circ\datedue.pm3-p.1

FINITE ELEMENT METHOD APPLIED TO DEFORMATION OF

METALLIC - GLASS RIBBON REINFORCED GLASS - CERAMIC MATRIX

COMPOSITE MATERIAL

By

John Dung Ninh

A THESIS

Submitted to
Michigan State University
in partial fulfillment of the requirements
for degree of

MASTER OF SCIENCE

Department of Metallurgy Mechanics and Material Science

1991

ABSTRACT

FINITE ELEMENT METHOD APPLIED TO DEFORMATION OF

METALLIC GLASS RIBBON REINFORCED GLASS - CERAMIC MATRIX

COMPOSITE MATERIAL

By

John Dung Ninh

The deformation characteristics of ceramic
composite material was studied numerically with the
objective of investigating the dependence of bending
properties on size, shape and distribution of the ribbon
reinforcing phase.

The model chosen for comparision was metallic
glass ribbon reinforced glass ceramic matrix composite.
The overall constitutive response of the composite and
the evolution of stress and strain field quantities in
the matrix of composite was computed using Finite Element
Method within the context of axisymetric and plane strain
unit cell formulations. The results indicate that the
development of significant stresses within a composite
matrix provides an important contribution to strengthening.

The numerical results provide a mechanistic
rationale for the experimentally observed trend for the
effect of ribbon on stress distribution within the composite.

AKNOWLEDGEMENTS

TABLE OF CONTENTS

LIST OF FIGURES

Page

LIST OF TABLES

INTRODUCTION

The effect of the ribbons on the crack growth in a brittle glass matrix has been investigated [1]. These composites, have been shown to have high longitudinal strength coupled with good off-axis properties [1]. Ribbon reinforcements unlike fiber reinforcements, possess the ribbon width as an additional geometrical parameter. Hence, the load transfer characteristics in the ribbon reinforced composites are expected to be influenced by ribbon's width. The ribbons can also be oriented differently with respect to their long and short transverse faces normal to the opening crack front.

Metallic materials, when reinforced with brittle fibers offer the potential for significant improvements in strength and toughness, particularly in mechanical performance over monolithic alloys. While metal matrix composites exhibit higher stiffness and strength than matrix alloys, they often suffer from lower ductility and inferior fracture toughness. Arguments for the strength and failure in the metal matrix composite are difficult, due to the lack of complete information on the processing, characterization and properties of the

materials. In a significant number of prior investigations, with which the composite properties are compared, the unreinforced matrix alloys, are obtained from different routes.

In this work, a chosen thickness of the metallic glass reinforcement in a glass ceramic matrix composite was studied by numerical analysis to gain a perspective on mechanics of strengthening. An understanding of this effect will be useful in optimizing the properties of such brittle matrix composites, in the attempt to make them suitable for structural applications.

The purpose of the finite element calculations is to measure changes in geometrical variables associated with the shape and distribution of the reinforcement.

1. Finite Element Method FEM.

FEM analysis was carried out using a Prime 750 or Unix computer system, and the program ANSYS, which is used for the solutions of several classes of engineering problems. The ANSYS element library offers 95 different element types to carry out a wide range of engineering analyses.

Element type STIFF 42 was used for analysis of metallic glass ribbon reinforced glass ceramic matrix composites. A mesh of elements is presented for ANSYS and FEM analysis, which is carried out with various numbers of ribbons. Dividing the area into a greater

number of elements increases the degree of accuracy.

2. Historical background.
    _____

Fischmeister and Sundstrom [2] used the FEM
technique to calculate stress-strain curves for different
hardness ratios between different phases present in
plain carbon steels (0.11 and 0.21 weight percent
carbon) and aluminum bronzes (8 to 12 percent aluminum).
They also studied the deformation of individual phase
regions in the case of plain carbon steel by using a two
dimensional model of the ferrite-martensite
microstructure.

Karlsson and Sundstrom [3] have also studied the
plastic deformation in ferritic-martensitic steels. They
used FEM to study inhomogeneity in the corresponding two
phase model.

Sundstrom [4] has used FEM to study the elastic
plastic behavior of WC-Co (tungsten carbide-cobalt)
alloys. He showed that the continuum mechanics can be
applied to a two dimensional model of real microstructure.
His results indicated that the plastic strain distribution
calculated by FEM is very inhomogeneous on a microscale
and FEM can not give the high resolution of stress and
strain fields in different phases.

Jinoch et. al. [5] used FEM to study the stress
and strain of alpha beta Ti-8Mn alloy. They used a
uniform mesh of 392 triangular two dimensional (plane

stress) plate elements. The volume fraction, particle
size and shape could be varied to designate each triangle
as either alpha or beta. The shapes of particles used
in meshes were not the same as those in actual specimens
but were idealized to make calculations simpler while
maintaining the volume fraction constant. Jinoch et. al.
showed that an FEM calculated stress-strain curve
attained lower stress levels for similar strain levels
as compared to an experimentally calculated stress-
strain curve . This difference may be due to the fine
grain sizes in Ti-8Mn alloy and the contributions of
the interface phase which were not considered in the FEM
calculations.

Margolin et. al. [6] studied the influence of
particle size, matrix and volume fraction of phases on
the stress and strain relationship of alpha beta Ti
alloys. They found that for a given volume fraction of
the second phase, the calculation of stress and strain
were higher for specimens with a finer particle size as
compared to those of specimens with coarser particle
size.

3. ANSYS program.
_____

ANSYS is a specific computer program, developed
and maintained by Swanson Analysis System Inc. It has
the ability to analyse static, dynamic, elastic, creep,
swelling, buckling, heat transfer, fluid, and current

flow problems . The program is based on the Finite
Element Method. ANSYS program gives results with high
degree of accuracy in a short period of computer time.
The program is very flexible and can be applied to many
engineering problems. ANSYS program includes three phases:
the preprocessing phase, the solution phase, and the
postprocessing phase.

a. Preprocessing phase.
_____

The preprocessing phase is carried out interactively;
the input is given directly and it may immediately provide
plots. The preprocessing phase begins with PREPn where n
is the number which dependes on the kinds of problems;
PREP7 for general purposes, PREP4 is for piping problem
etc, and the preprocessing phase may include many PREPn
as the subroutines.

b. Solution phase.
_____

The solution phase checks the data before program
progressed to the actual execution. The solution phase
does not provide the solutions; it interprets the data
input and, checks elements, and various levels of
program. If there were errors, it would produce the
errors in this phase.

c. postprocessing phase.
_____

The postprocessing phase consists of several

modules. Each module performs a different operation
and contains a unique set of commands. The postprocessing
phase will give the solutions, the plots and it stores
data to use for next time.

4. Description of analysis.
_____

The overall equilibrium equations for static
analysis are

$$[K] \{ u \} = \{ F \}$$

or

$$[K] \{ u \} = \{ F1 \} + \{ F2 \}$$

where

[K] is total stiffness matrix = total element
stiffness matrix.

{ u } is nodal displacement vector

{ F1 } is reaction load vector, and

{ F2 } is total applied load vector.

The stress sigma is related to the strain epsilon by

$$\{ sigma \} = [D](\{ epsilon \} - \{ epsilon1 \})$$

where

[D] is elasticity matrix.

{ epsilon1 } is thermal strain vector.

The element stresses are computed by

$$\{ sigma \} = [D]([B]\{ u \} - \{ epsilon1 \})$$

because

$$\{ epsilon \} = [B]\{ u \}$$

where

[B] is strain displacement matrix which must be

specified for each stress calculation point, and

{ u } is nodal displacement.

5. The aim of this project.
   _____

The aim of this project is to study the effect of different ribbon configurations on the stress distribution in ribbon reinforced brittle ceramic matrix composite by using two dimensional Finite Element Method.

PROCEDURE OF FINITE ELEMENT ANALYSIS

1. Composite system.
_____

The specimens considered in this study were
fabricated using Corning glass code 7572 (code numbers
of products of Corning Glass Company) as the matrix
material. An iron based metallic glass METGLAS 2605 S - 2
(registered trademark of Allied Signal Inc. for amorphous
metallic alloys and brazing alloys) alloy was used as
the reinforcement [1].

The physical properties and chemical compositions
of metallic glass and ceramic glass matrices are presented
in tables I and II. The volume fraction of the ribbons
(0.8) was kept constant in all of the samples studied
by FEM. This was achieved by changing the thickness
(subdividing) but keeping the width and length the same.

The residual stress induced by the thermal
expansion coefficient between the matrix and
reinforcement was small and could be neglected since

coefficient of matrix   = 95 x 10E-7 per degree

coefficient of ribbon   = 76 x 10E-7 per degree.

Strong bonding was observed between ribbon and

matrix. The ribbon geometries used in the modelling varied as

40 mm x 50 mm x 8 mm for one ribbon.

40 mm x 50 mm x 4 mm for two ribbons.

40 mm x 50 mm x 2 mm for four ribbons.

40 mm x 50 mm x 1 mm for eight ribbons.

40 mm x 50 mm x 0.5 mm for sixteen ribbons.

The dimension of the composite specimen was

40 mm x 50 mm x 10 mm .

Experimental verification of the predictions based on FEM analysis were carried out with specimens prepared by using the following steps [7]:

   a. Specimen was wet pressed in a steel die,

   b. And then compacted at 3000 Psi (21 MPa)

   c. The specimen was next preheated to 250 degree C for 15 minutes to drive off the organic binder,

   d. Then sintered at 400 degree C for 90 minutes.

   e. Then it was treated at 450 degree C for 20 minutes for matrix crystallization as recommended by manufacturer,

   f. And cooled to room temperature within the furnace in order to minimize thermal shock.

The main crystalline phase was 2PbO.ZnO, and the specimens were tested in three point bending using an Instron machine with a crosshead speed of 0.05 cm / min.

2. Finite Element Method (FEM).

FEM was used to calculate the stress distributions in the specimens.

The meshes were provided to the ANSYS program. In the finite element model, the nodes A and B can move only in the X-direction. Node C can move in the Y-direction. The other nodes can move in both X and Y-directions. A force of 125 N (load corresponding to fracture strength of the matrix of the selected size) was applied to node C, normal to the ribbons, as shown in Figure 1.

TABLE I

Properties of metallic glass ribbon [7].

Property	Metglas 2605 S-2
Chemical composition w/o	Fe 78 B 13 Si 9
Crystallization temperature	550
Elastic modulus (GPa)	85
Yield strength (MPa)	> 700
Coefficient of thermal expansion (degree C^{-1})	76×10^{-7}
Density (g cm^{-3})	7.18

TABLE II

Properties of ceramic glass matrix [7].

Property	:	Corning glass 7572
Softening point (degree C)	:	375
Coefficient of thermal expansion (degree C $^{-1}$)	:	95×10^{-7}
Density (g cm $^{-3}$)	:	6
Elastic modulus (GPa)	:	33.4
Continuous service temperature (degree C)	:	450
Chemical composition (w/o)	:	PbO 70 B_2O_3 5 - 10 SiO_2 2 - 5 Al_2O_3 1 - 5 ZnO 10 - 20

FIGURE 1.

_____

Specimen model.

- Darker segments are ribbons.

- Lighter segments are matrix.

- Nodes A and B move in X direction only.

- Node C moves in Y direction only.
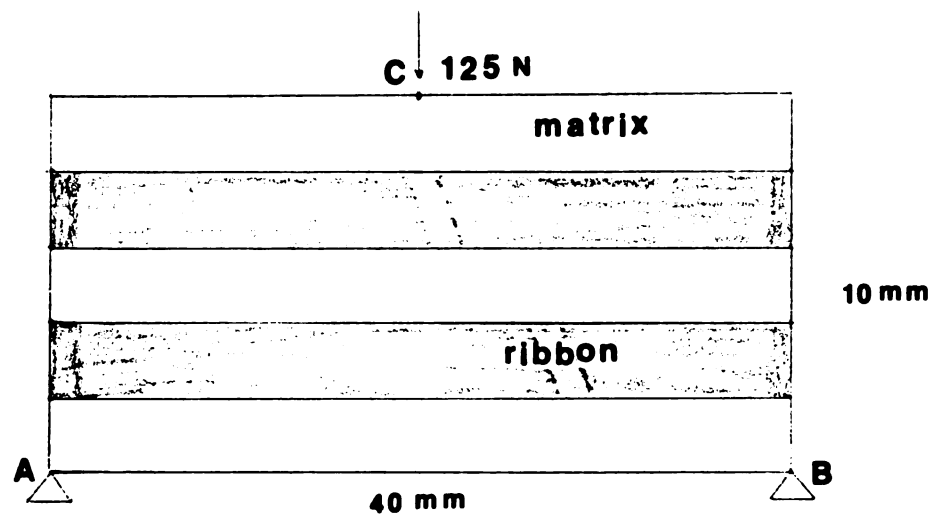
3. Finite elements models.

In the first case, the specimen was reinforced
with one ribbon (8 mm thick), as shown in Figure 2.
There were two symmetric parts, the dark and light parts.
Each part included one matrix segment that was divided
into smaller triangular elements, and another half of
thickness of the ribbon which was divided into larger
triangular elements.

The composite specimen was analysed by using 256
triangular elements and 177 nodes. Both the matrix
segments, and the ribbon segments consisted of 128
elements. The thickness of the matrix segment was
divided into two parts located on either side of ribbon,
each part having a thickness of 1 mm. The ribbon segment
was 8 mm thick . The length of the specimen was 40 mm,
and was divided into 17 equi-distant nodes. The nodes
were numbered in an increasing order in the horizontal
direction. The number of the node increased by 20 for
each step in the vertical direction.

For the second case, the specimen was reinforced with
two ribbons as shown in Figure 3. There were three
matrix segments and two ribbon segments. As in the first
case, the matrix segments were divided into the smaller
triangular elements and the ribbon segments were divided
into larger triangular elements. The composite specimen

was analysed by using 320 triangular elements and 217 nodes.

In this case, each matrix segment was 0.66 mm thick, while each ribbon segment had a thickness 4 mm. The length of the specimen was 40 mm, and was divided into 17 equi-distant nodes. Node numbering was carried out in a fashion similar to the one described in the previous case.

In the third case, the specimen was reinforced with four ribbons. There were five matrix segments and four ribbon segments, as shown in Figure 4. The composite specimen was analysed using 576 elements and 377 nodes.

In this case, each matrix segment was 0.4 mm thick, while each ribbon segment was 2 mm thick. The length of the specimen was 40 mm, and was divided into 17 equi-distant nodes.

For the fourth case, the specimen was reinforced with eight ribbons as shown in Figure 5. There were nine matrix segments and eight ribbon segments. In this case, the composite specimen was analysed by using 1088 elements and 697 nodes.

Each matrix segment at either surface of the specimen was 0.3 mm thick, while the other matrix segments had a thickness of 0.2 mm. Each ribbon segment was 1 mm thick. The length of the specimen was 40 mm and was divided into 17 equi-distant nodes.

In the last case, the specimen was reinforced with

sixteen ribbons; there were 17 matrix segments and 16 ribbon segments, as shown in Figure 6. The specimen was analysed by using 528 elements and 677 nodes.

Each matrix segment at either surface of the specimen was 0.175 mm thick. The other matrix segments had a thickness of 0.11 mm. Each ribbon segment was 0.5 mm thick. The length of the specimen was 40 mm and was divided into 17 equi-distant nodes.

FIGURE 2.

      Finite element model of specimen

reinforced with one ribbon.

      - Small triangles are in matrix element.

      - Large triangles are in ribbon element.

ANSYS 4.4A
MAR 3 1991
11:41:32
PLOT NO.   1
PREP7 ELEMENTS
TYPE NUM

XV =1
ZV =1
DIST=15.557
XF =20
YF =5
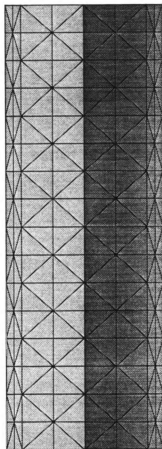
ONE RIBBON

FIGURE 3.
_____

      Finite element model of specimen

      reinforced with two ribbons.

      - Small triangles are in matrix element.

      - Large triangles are in ribbon element.

21

ANSYS 4.4A
MAR 3 1991
12:50:52
PLOT NO. 1
PREP7 ELEMENTS
TYPE NUM

XV =1
ZV =1
DIST=15.557
XF =20
YF =5

TWO RIBBONS

FIGURE 4.
_____

      Finite element model of specimen

      reinforced with four ribbons.

      - Small triangles are in matrix element.

      - Large triangles are in ribbon element.

ANSYS 4.4A
MAR 14 1991
15:59:42
PLOT NO. 1
PREP7 ELEMENTS
TYPE NUM

XV =1
ZV =1
DIST=15.557
XF =20
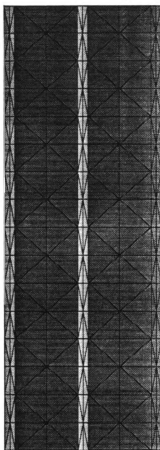YF =5

FOUR RIBBONS

FIGURE 5.
_____

       Finite element model of specimen

       reinforced with eight ribbons.

       - Small triangles are in matrix element.

       - Large triangles are in ribbon element.

ANSYS 4.4A
MAR 14 1991
18:59:42
PLOT NO.   1
PREP7 ELEMENTS
TYPE NUM

XV =1
ZV =1
DIST=15.557
XF =20
YF =5

EIGHT RIBBONS

FIGURE 6.
_____
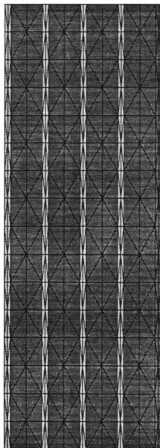
       Finite element model of specimen

reinforced with sixteen ribbons.

  - Small rectangles are in matrix element.

  - Large rectangles are in ribbon element.

ANSYS 4.4A
MAR 14 1991
21:10:14
PLOT NO. 1
PREP7 ELEMENTS
TYPE NUM

XV =1
ZV =1
DIST=15.557
XF =20
YF =5
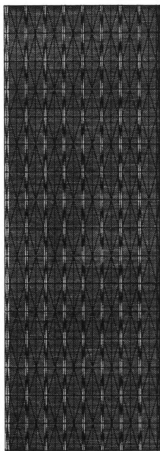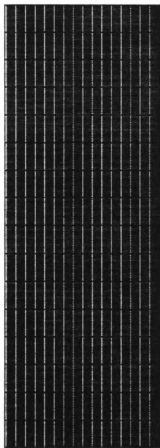
SIXTEEN RIBBONS

RESULTS AND DISCUSSIONS

The maximum tensile stress in the outer fiber (before failure of the matrix) of the sample (in three point bending) is given by

$$\text{sigma} = 3PL / 2bd^2$$

where

sigma is fracture strength of the matrix

P is required force

L is length of composite = 40 mm

b is width of composite = 50 mm, and

d is thickness of composite = 10 mm.

The first crack in the matrix will form when the outer fiber stress reaches the matrix fracture stress.

The load for failure of the specimen considered was calculated as

$$P = 2bd^2 \text{sigma} / 3L = 125 \text{ N}.$$

The stress in the matrix segments was determined by the FEM analysis. The stress in each matrix segment was determined at the load where the first matrix crack would be initiated on the tensile surface corresponding to the fracture stress of the matrix (= 15 MPa).

1. The analysis of the stress distribution.

a.   Specimen reinforced with one ribbon.

The stress distribution in the specimen reinforced
with one ribbon is shown in Figure 7. The stress was
compressive in the upper half, while it was tensile in
the lower half. The stress was close to zero (2.014 MPa)
at the neutral surface. The maximum tensile stress is in
the darkest region which has the value of 59.846 MPa. The
maximum compressive stress is in the lightest region, and
had a value -70.276 MPa. The stress slowly increased
from the maximum tension to maximum compression from the
lower to the upper part of specimen. The stresses are
also reduced at the nodes laterally far-distanced from
the middle nodes.

With the values of stress distribution given by
ANSYS, and the fracture strength of the matrix (15 MPa)
one can predict the number of cracked matrix segments.
The matrix segments would be cracked when the value of
stress distribution on it is greater than 15 MPa. The
matrix segment will be uncracked when the value of stress
distribution is lower than 15 MPa. In Figure 7, the crack
might occur in the lower matrix segment, and the shortest
length of cracked line is 1 mm.

b. Specimen reinforced with two ribbons.

_____

The stress distribution in the specimen reinforced
with two ribbons is shown in Figure 8. The stress is
compressive in the upper half, while it is tensile in
the lower half. The maximum tensile stress is 60.892 MPa
in the darkest region, and the maximum compressive
stress is -73.68 MPa in the lightest region. The stress
was close to zero (1.082 MPa) at the neutral surface.
The values of stress slowly decreased from the darkest
region to lightest region; stress also decreased at the
nodes laterally far-distanced from the middle nodes. With
the values of stress distribution given by ANSYS, and the
fracture strength of the matrix (15 MPa), one can
predict the number of cracked matrix segments. The matrix
segments would be cracked when the value of stress on it
is greater than 15 MPa. They will be uncracked when the
value of stress is lower than 15 MPa. In Figure 8, The
crack might occur in the lowest matrix segments and the
shortest length of cracked line is 0.66 mm.

c. Specimen reinforced with four ribbons.

_____

The stress distribution in the specimen reinforced
with four ribbons is shown in Figure 9. The stress is
compressive in the upper half, while it is tensile in
the lower half. The maximum tensile stress is 63.644 MPa
in the darkest region, and the maximum compressive stress

is -78.962 MPa in the lightest region. The values of
tensile and compressive stresses reduced from the darkest
region to the lightest region, and at the nodes laterally
far-distanced from the middle nodes. The stress was close
to zero (0.253617 MPa) at neutral surface.

With the value of stress distribution given by the
ANSYS, and the fracture strength of the matrix (15 MPa),
one can predict the number of cracked matrix segments.
The matrix segments would be cracked when the value of
stress distribution on it is greater than 15 MPa. They
will be uncracked when the value of stress distribution
is lower than 15 MPa. In Figure 9, the crack might occur
in the two lowest matrix segments, and the total shortest
length of the cracked line will be 0.8 mm.

d. Specimen reinforced with eight ribbons.
_____

The stress distribution in the specimen reinforced
with eight ribbons is shown in Figure 10. The stress is
compressive in the upper half, while it is tensile in
the lower half. The maximum tensile stress is 64.474
MPa in the darkest region. The maximum compression stress
region is - 80.555 MPa in the lightest region. The values
of stress were reduced from the darkest region to the
lightest region, and at the nodes laterally far-distanced
from the middle nodes. The stress was close to zero
(0.0166 MPa) at the neutral surface.

With the value of stress distribution given by

ANSYS, and the fracture strength of the matrix (15 MPa),
one can predict the number of cracked matrix segments.
The matrix segements would be cracked when the value of
stress distribution on it is greater than 15 MPa. They
will be uncracked when the value of stress distribution
is lower than 15 MPa. In Figure 10, the crack might occur
in the four lowest matrix segments, and the total
shortest length of cracked line will be 0.9 mm.

e. Specimen reinforced with sixteen ribbons.

The stress distribution in the specimen reinforced
with sixteen ribbons is shown in Figure 11. The stress
is compressive in the upper half, while it is tensile
in the lower half. The maximum tensile stress is 70.299
MPa in the darkest region, and the maximum compressive
stress is - 95.524 MPa in the lightest region. The value
of stress reduced from the darkest region to the lightest
region, and at the nodes laterally far-distanced from
the middle nodes. The stress is close to zero at the
neutral surface.

With the values of stress distribution given by
ANSYS, and the fracture strength of the matrix (15 MPa),
one can predict the number of cracked matrix segments.
The matrix segment would be cracked when the value of
stress distribution on it is greater than 15 MPa. They
will be uncracked when the value of stress is lower than
15 MPa. In Figure 11, the crack might occur in the lowest

seven matrix segments, and the total shortest length of the cracked line will be 0.835 mm.

A comparison of specimens with one, two, four, eight, and sixteen ribbons, provides the following results:

- The magnitude of stress increases at the regions far-distanced from the neutral surface of the specimen, and decreases at the nodes laterally far-distanced from the middle nodes.

- The maximum value of outer fiber tensile stress was lowest in the specimen with one ribbon 59.846 MPa; this value increased in the specimens having more ribbons, as in the specimen with sixteen ribbons the maximum tensile stress was 70.299 MPa.

- The maximum value of compressive stress region was lowest at the specimen with one ribbon - 70.276 MPa; this value increased in the specimens having more ribbons as in the specimen with sixteen ribbons, the maximum compressive stress was - 95.524 MPa.

So the maximum values of tensile and compressive stresses increase with increasing number of ribbons.

FIGURE 7.
_____

Stress distribution for specimen

reinforced with one ribbon.

- Positive number is the value

of tensile stress.

- Negative number is the value

of compressive stress.

- Small triangles are in matrix element.

- Large triangles are in ribbon element.

- MN is middle nodes.

ANSYS 4.4A
MAR 3 1991
11:08:17
PLOT NO. 1
POST1 STRESS
STEP=1
ITER=1
SX   (AVG)
S GLOBAL
DMX =0.071025
SMN =-70.276
SMNB=-101.358
SMX =59.846
SMXB=69.235

XV =1
ZV =1
DIST=15.557
XF =20
YF =5

-70.276
-55.818
-41.36
-26.902
-12.444
2.014
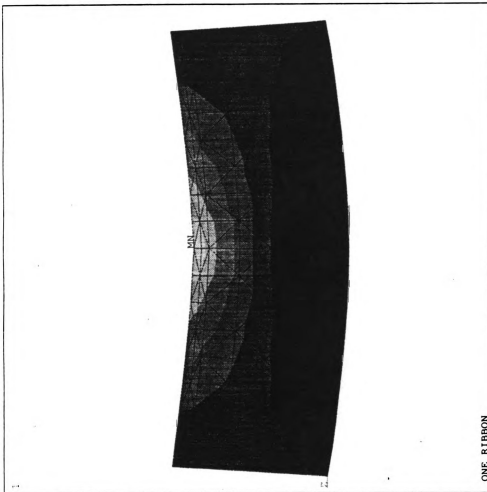16.472
30.93
45.388
59.846

ONE RIBBON

FIGURE 8.

———————

Stress distribution for specimen

reinforced with two ribbons.

- Positive number is the value

  of tensile stress.

- Negative number is the value

  of compressive stress.

- Small triangles are in matrix element.

- Large triangles are in ribbon element.

- MN is middle nodes.

ANSYS 4.4A
MAR 3 1991
12:15:51
PLOT NO. 1
POST1 STRESS
STEP=1
ITER=1
SX (AVG)
S GLOBAL
DMX =0.070948
SMN =-73.68
SMNB=-107.202
SMX =60.892
SMXB=69.425

XV =1
ZV =1
DIST=15.557
XF =20
YF =5
    -73.68
    -58.728
    -43.775
    -28.823
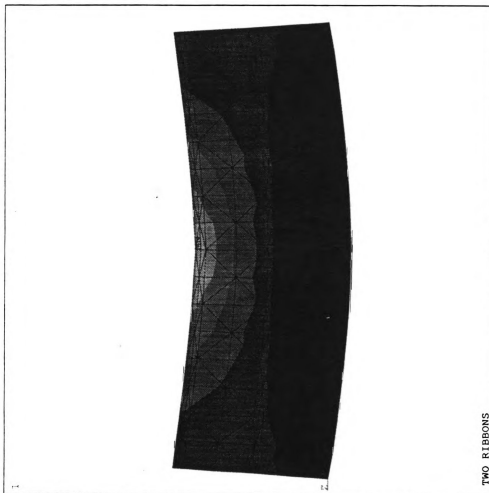   -13.87
    1.082
    16.035
    30.987
    45.94
    60.892

TWO RIBBONS

FIGURE 9.
_____

      Stress distribution for specimen

reinforced with four ribbons.

- Positive number is the value

  of tensile stress.

- Negative number is the value

  of compressive stress.

- Small triangles are in matrix element.

- Large triangles are in ribbon element.

- MN is the middle nodes.

39

ANSYS 4.4A
MAR 8 1991
16:02:08
PLOT NO. 1
POST1 STRESS
STEP=1
ITER=1
SX (AVG)
S GLOBAL
DMX =0.072525
SMN =-78.962
SMNB=-114.029
SMX =63.644
SMXB=71.649

XV =1
ZV =1
DIST=15.557
XF =20
YF =5

-78.962
-63.117
-47.272
-31.426
-15.581
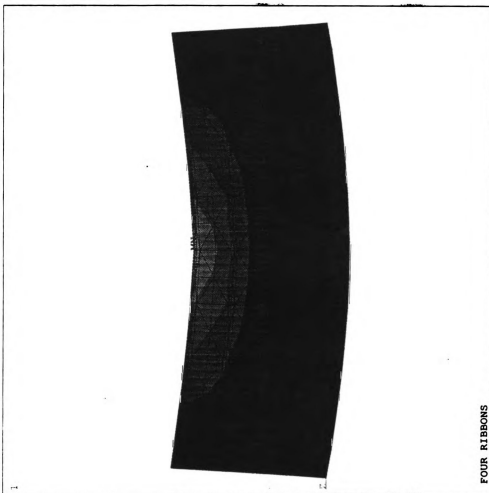0.263617
16.109
31.954
47.799
63.644

FOUR RIBBONS

FIGURE 10.
_____

Stress distribution for specimen

reinforced with eight ribbons.

- Positive number is the value

of tensile stress.

- Negative number is the value

of compressive stress.

- Small triangles are in matrix element.

- Large triangles are in ribbon element.

- MN is the middle nodes.

ANSYS 4.4A
MAR 14 1991
17:04:23
POST1 STRESS
PLOT NO. 1
STEP=1
ITER=1
SX   (AVG)
S GLOBAL
DMX =0.072791
SMN =-80.555
SMNB=-116.176
SMX =-64.474
SMXB=72.484

XV =1
ZV =1
DIST=15.557
XF =20
YF =5
        -80.555
        -64.441
        -48.327
        -32.212
        -16.098
        0.016636
        16.131
        32.245
        48.36
        64.474

EIGHT RIBBONS

FIGURE 11.

_____

       Stress distribution for specimen

reinforced with sixteen ribbons.

   - Positive number is the value

      of tensile stress.

   - Negative number is the value

      of compressive stress.

   - Small rectangles are in matrix element.

   - Large rectangles are in ribbon element.

   - MN is the middle nodes.

ANSYS 4.4A
MAR 14 1991
20:06:40
PLOT NO.   1
POST1 STRESS
STEP=1
ITER=1
SX   (AVG)
DMX =0.080818
SMN =-95.524
SMNB=-124.75
SMX =70.299
SMXB=73.911

XV =1
ZV =1
DIST=15.557
XF =20
YF =5

-95.524
-77.099
-58.674
-40.25
-21.825
-3.4
15.025
33.45
51.874
70.299

SIXTEEN RIBBONS
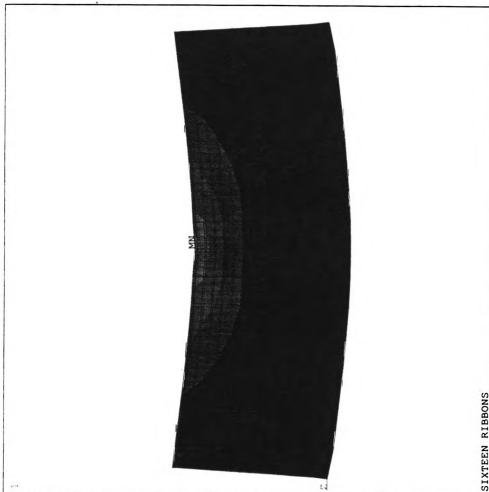
2. Analysis of the plots.

Fraction of cracked matrix segments can be defined as the ratio of number of layers of matrix that are cracked divided by the total number of matrix layers Figure 12, is a plot of fraction of cracked matrix segments versus number of ribbons ' n '. A plot relating number of cracked segments to the number of ribbons is provided in Figure 13.

Another point of interest is to learn how stress varies at various locations along a vertical section. For this purpose, node number 9; the lowest node in the mid section (in the tensile region) is chosen as the origin as shown in Figure 14, and the distances of all other middle nodes are measured relative to this origin. The plots of stresses in the middle nodes versus the distances of these nodes from the origin are shown in Figures 15, 16, 17, and 18. The zero stress at the neutral surface, and its location do not depend on the number of ribbons in the specimens as shown in Figure 19.

FIGURE 12.

_____

      The plot of fraction of cracked matrix

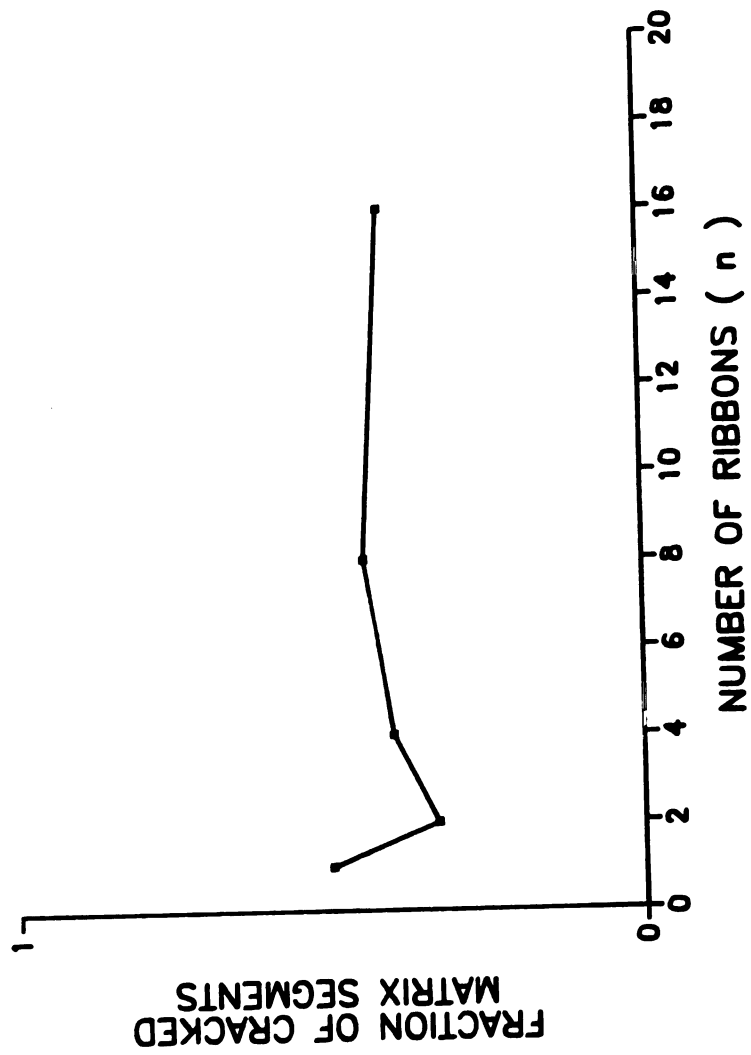   segments versus total number of ribbons.

46

FRACTION OF CRACKED
MATRIX SEGMENTS

NUMBER OF RIBBONS (n)

FIGURE 13.

_____

The plot of total number of cracked matrix

segments versus number of ribbons.
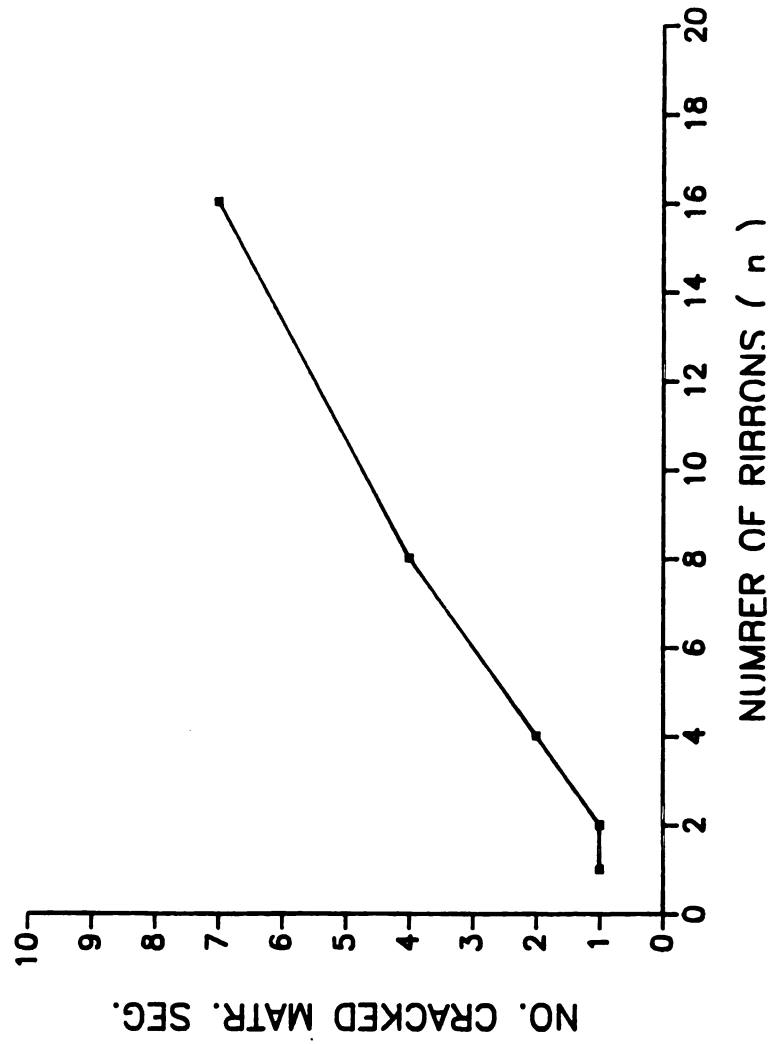
NUMRER OF RIRRONS (n)

NO. CRACKED MATR. SEG.

FIGURE 14.

_____

       Schematic illustrating location of

middle nodes relative to the origin.

- Node number 9 is the origin.

- Dots indicated are middle nodes.

- Nodes A and B move in X direction only.
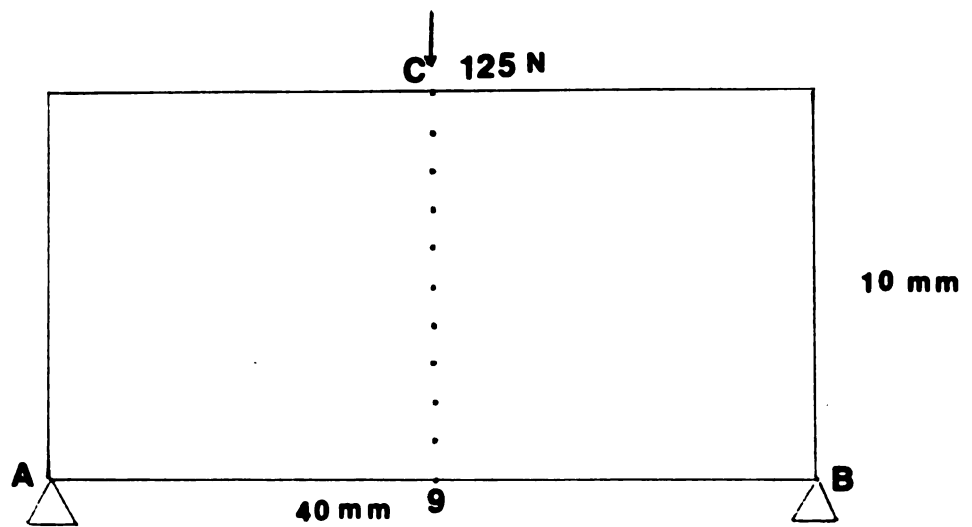
- Node C moves in Y direction only.

FIGURE 15.
_____

The plot of stress versus distance of nodes

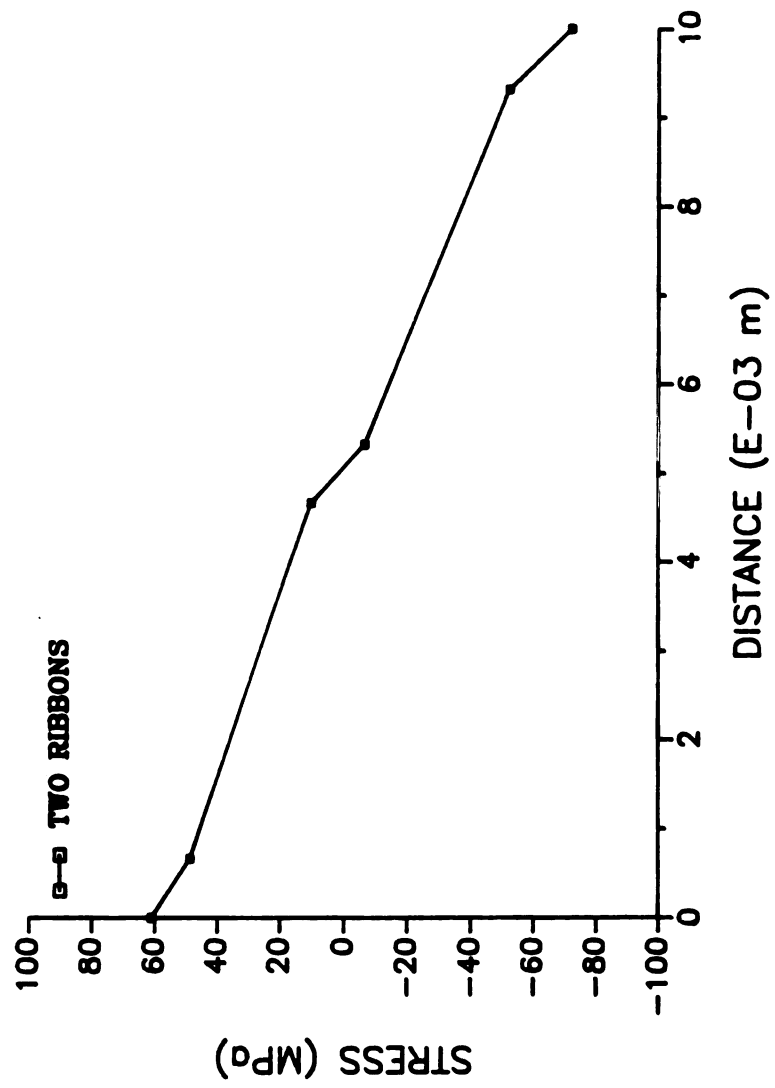to the origin in specimen reinforced

with two ribbons.

FIGURE 16.
_____

The plot of stress versus distance of

nodes to the origin in the specimen
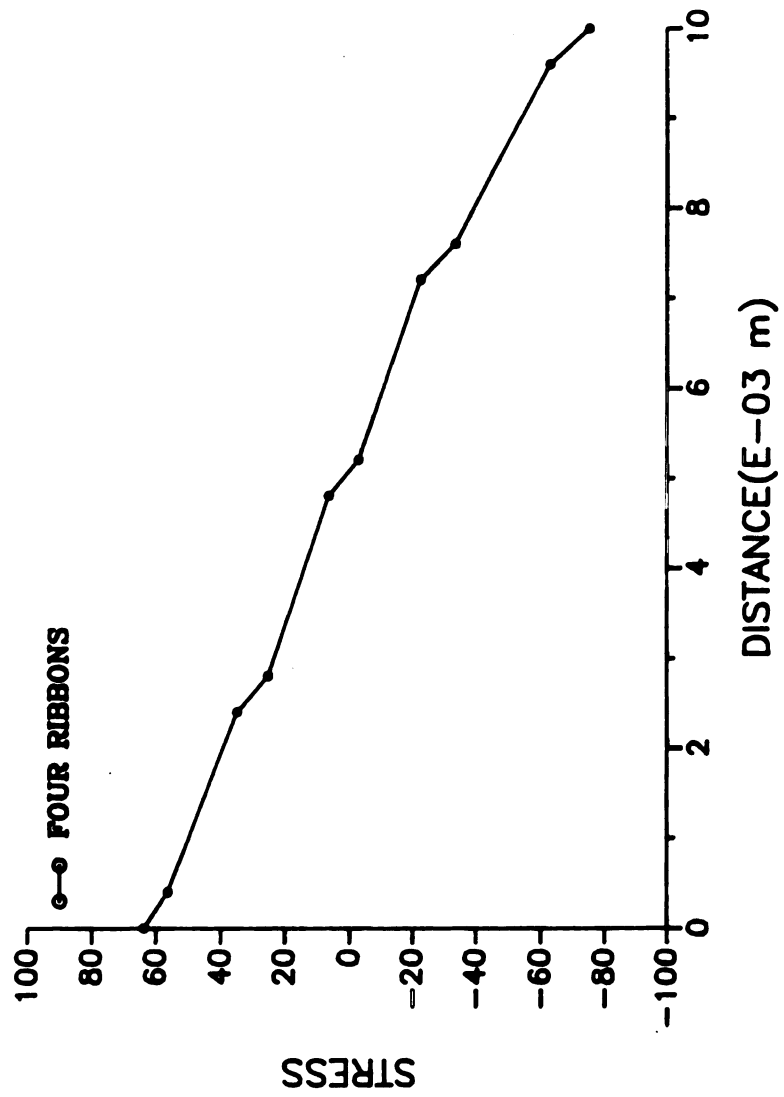
reinforced with four ribbons.

54

FIGURE 17.

_____

       The plot of stress versus distance of

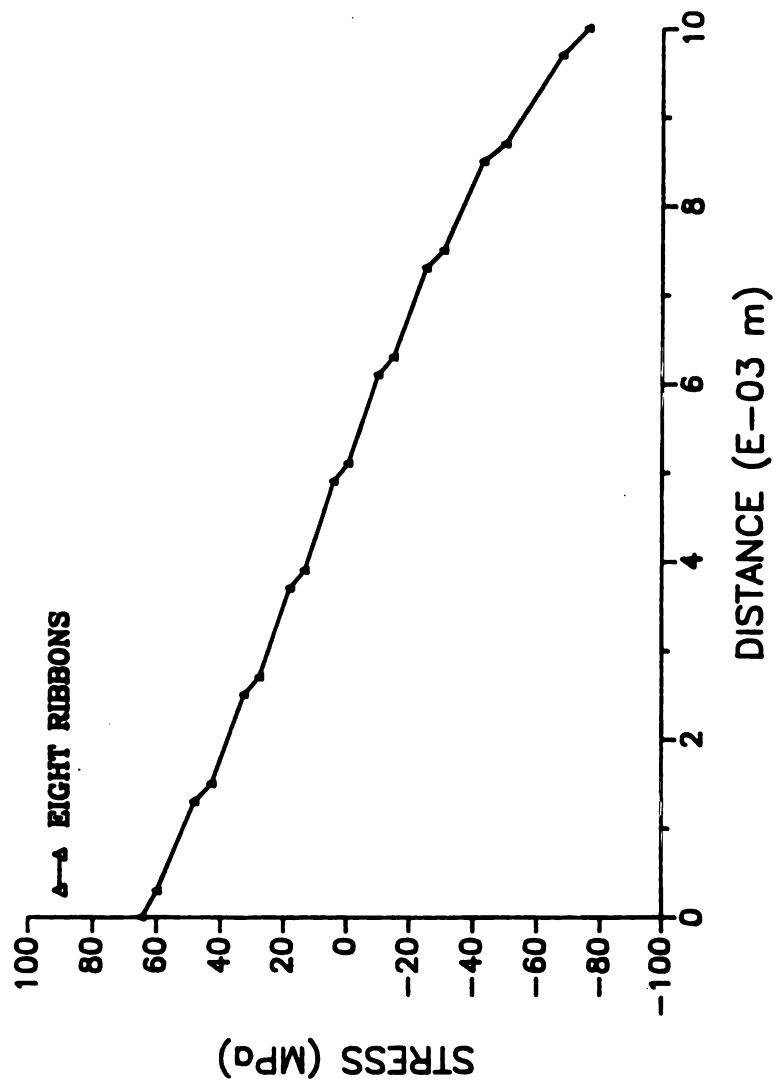   nodes to the origin in the specimen

       reinforced with eight ribbons.

FIGURE 18.

The plot of stress versus distance of

nodes to the origin in the specimen
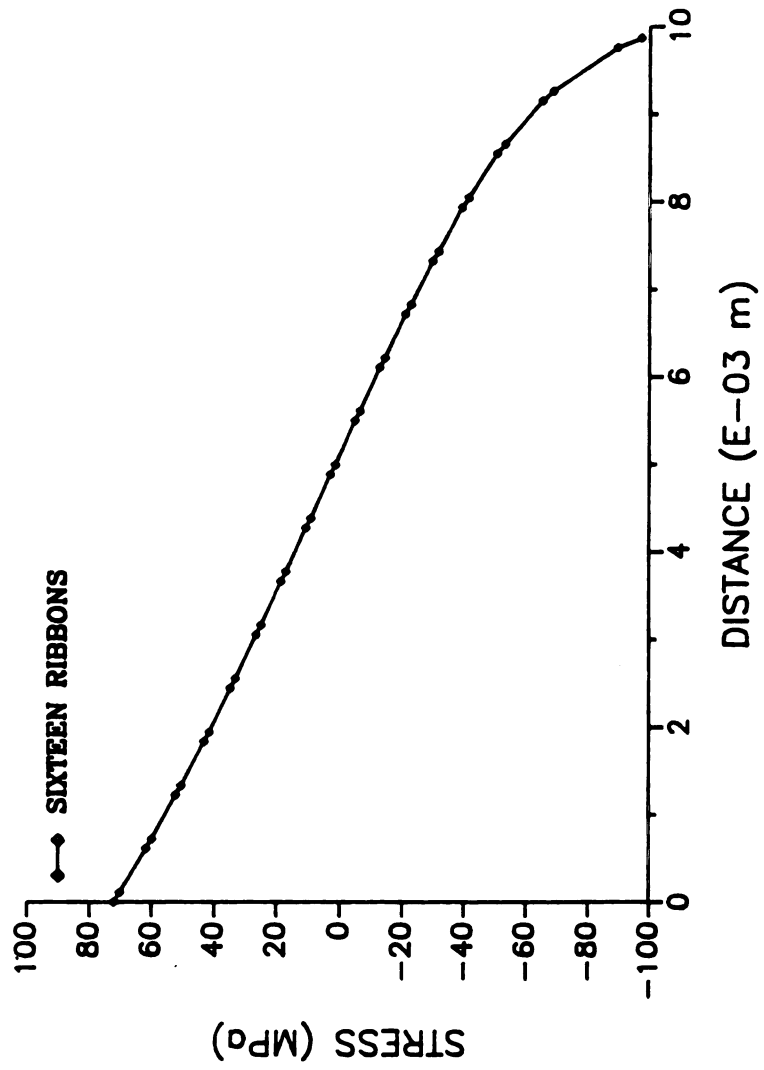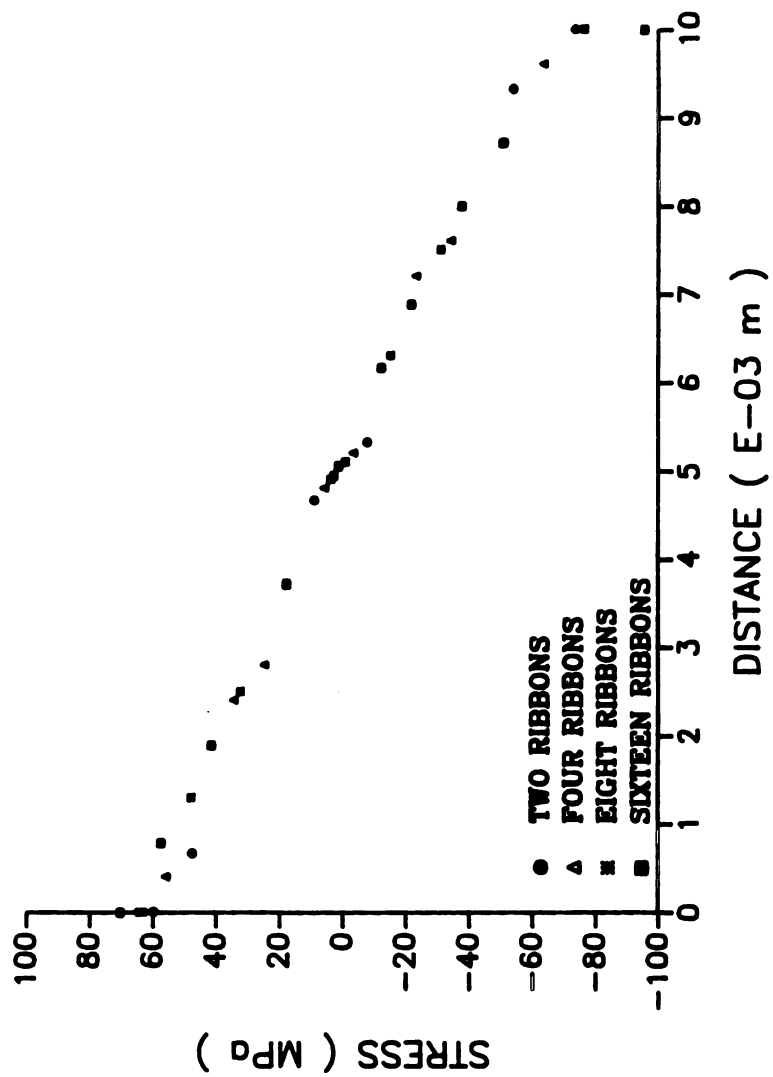
reinforced with sixteen ribbons.

SIXTEEN RIBBONS

STRESS (MPa)

DISTANCE (E-03 m)

FIGURE 19.

_____

> The plot of stress versus distance of nodes
>
> to the origin in the specimens reinforced
>
> with two, four, eight, and sixteen ribbons.

60

The following is the summary of results drawn from this study:

- The ribbon distribution had a significant effect on the stress distribution in the composite specimen. This can be seen in Figures 7, 8, 9, 10, and 11, for specimens with 1, 2, 4, 8, and 16 ribbons respectively.

- From the stress distribution the segments of the matrix that would crack instantly can be determined. This was achieved by comparing the magnitude of the stresses (tensile) to the cracking stress of the matrix (in tension and ignoring coupling effects).

A generalized empirical value for the number of cracked segments in a composite with ' n ' ribbons is

$$\log_2 (n) - 1 \quad .$$

Hence the number of uncracked matrix segments is

$$(n + 1) - 2^{\log (n) - 1} \quad .$$

Even when some matrix segments are cracked, few remaining matrix segments do continue to contribute to the overall composite strength (along with the ribbons). The total composite strength sigma1 remaining can be expressed as.

$$sigma1 = (sigma2 \ X \ V2) + \ K \ (sigma3 \ X \ V3)$$

where K is a fraction depending on the number of uncracked matrix segments. The value of K varies with ' n ' and is equal to

$$K = (n+1) - 2^{\log(n)-1} / (n+1)$$

and hence

$$\text{sigma1} = (\text{sigma2} \times V2) + ([(n+1) - 2^{\log(n)-1}]$$
$$/ (n+1)) \times (\text{sigma3} \times V3).$$

The strength for composites having (same volume fraction of ribbons) various numbers of ribbons can be given as

sigma1 = (sigma2 X V2) + 1 / 2 (sigma3 X V3) for n = 1

sigma1 = (sigma2 X V2) + 2 / 3 (sigma3 X V3) for n = 2

sigma1 = (sigma2 X V2) + 3 / 5 (sigma3 X V3) for n = 4

sigma1 = (sigma2 X V2) + 5 / 9 (sigma3 X V3) for n = 8

sigma1 = (sigma2 X V2) + 10 / 17(sigma3 X V3) for n = 16.

From the results it is evident that the matrix contribution to the strength is fairly constant (of the order of 50 % to 60 %) indicating that only 50 % to 60 % of the matrix contributes to the strength at any instant (after the first crack in matrix region has been initiated). Such a behavior has also been observed experimentally for the cases with 1, 2 and 4 ribbons. Experimental verification of prediction of number of cracked segments based on FEM analysis for these cases has been good.

This type of information is particularly useful when incorporating such composites for practical applications. Although the first matrix crack governs

the resulting properties of the composite, the load that the composite can carry does not decrease significantly when the first matrix crack appears if sigma2 >> sigma3 . A typical load displacement curve for such a composite is shown in the Figure 20.

Modelling studies can be carried out incorporating practical conditions. The results based on such studies can affect the decision to use or discard any given component once a certain fraction of the matrix has cracked.

Another important point which has to be accounted for is the constantly changing position of the neutral axis in a dynamic test. The results obtained in the present study are only useful under static conditions (constant load). Any dynamic loading can alter the conditions dramatically and change the end results.

FIGURE 20.

_____

The plot of load versus displacement
of composite specimen.

- Number 1 indicates the position where the
  first matrix segment crack occurs.

- Number 2 indicates the position where the
  load is carried by ribbons and uncracked
  matrix segments.

- Number 3 indicates the position where the
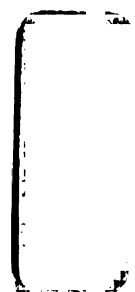 composite failure occurs.
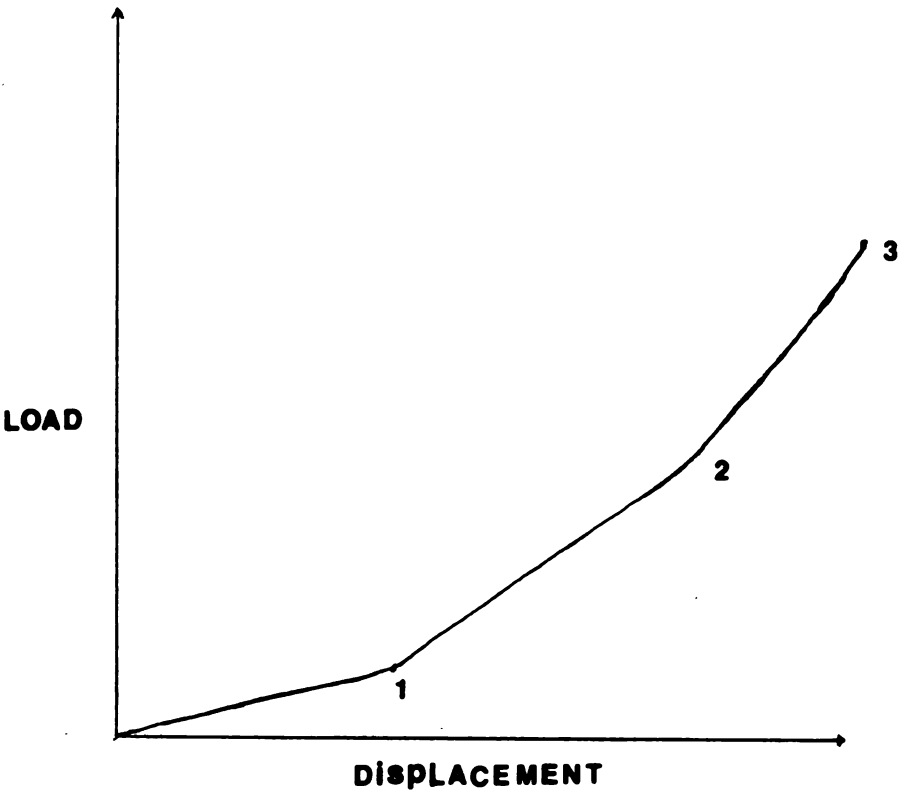
SUMMARY

For a given volume fraction of ribbon reinforcement, the ribbon distribution (number of ribbons) affects the stress distribution; however, it does not significantly change the fraction of cracked matrix segments. This behavior indicates that the number of the ribbons would not alter the end results, provided the volume fraction is kept constant. Hence, based on practical constraints, it would be beneficial to incorporate fewer ribbons rather than more narrower ones.

IV.   REFERENCES

1. Rajendra U. Vaidya and K. N. Subramanian,
    " Effect of Ribbon Orientation on Fracture Toughness
    of Metallic-Glass Ribbon Reinforced Glass-
    Ceramic Matrix Composite, " J. Am. Ceram. Soc.,
    73, 2962 (1990).

2. H. Fischmeister, J. Hjalmered, B. Karlsson,
    G. Lindon and B. Sundstrom,
    Third international conference on strength of
    materials and alloys, Institute Metals, and Iron
    and Steel Institute,
    Cambridge and London, 1, 621 (1973).

3. B. Karlsson and B. Sundstrom, " Inhomogeneity in
    Plastic Deformation of Two Phase Steel, "
    Mat. Sci. Eng., 17, 161 (1974)

4. B. Sundstrom, " Elastic Plastic Behavior of WC-Co
    Analyzed by Continuum Mechanics, " Mat. Sci. Eng.,
    12, 265 (1973).

5. J. Jinoch, S. Ankem and H. Margolin, " Calculation
    of Stress-Strain Curve and Stress- Strain
    Distribution for Alpha-Beta Ti-8Mn Alloy, "
    Mat. Sci. Eng., 34, 203 (1978).

6. S. Ankem and H. Margolin, " FEM Calculations of Stress-Strain Behavior of Alpha-Beta Ti-Mn Alloy, " Metall. Trans. A., 13, 95 (1982).

7. Rajendra U. Vaidya and K. N. Subramanian, " Metallic-Glass Ribbon Reinforced Glass- Ceramic Matrix Composite, " J. Mat. Sci., 25, 3291 (1990).

8. T. Christman, A. Needleman and S. Suresh, " An Experimental and Numerical Study of Deformation in Metal-Ceramic Composites, " Acta. Metall., 37, 3029 (1989).

9. Sagar P. Naik, " Role of the phase boundary on deformation of polycrystalline Alpha - Beta brass, " Master thesis, M.S.U., E. Lansing Michigan (1985).

10. Peter C. Kohnke and J. Swanson, ANSYS Engineering Analysis System -- Theoretical manual, Swanson Analysis System, Inc., Houston, PA.

11. Gabriel J. Desalvo and J. Swanson, ANSYS Engineering Analysis Systems -- User 's manual, 1, Swanson Analysis Systems, Inc., Houston, PA.

12. Gabriel J. Desalvo and J. Swanson, ANSYS Engineering Analysis Systems -- User 's manual, 2, Swanson Analysis Systems, Inc., Houston, PA.

13. Gabriel J. Desalvo, ANSYS Engineering Analysis Systems -- Verification, Analysis Systems, Inc., Houston, PA.

14. J. Swanson, ANSYS Engineering Analysis Systems -- Examples, Swanson Analysis Systems, Inc., Houston, PA.

15. Margaret Wilke and Jackie Carlson, User 's guide, Case Center Coll. Eng. Mich. Sta. Uni.

16. Lary J. Segerlind, Applied Finite Element Analysis, John Wiley and Sons Inc. New York (1984).

17. J. N. Reddy, An introduction to the Finite Element Method, McGraw Hill Inc. New York (1984).